Stability of the Sonoluminescing Bubbles

Ljubinko Kondić*
Courant Institute of Mathematical Sciences, New York University
New York City, NY 10012

Joel I. Gersten
City College of The City University of New York
New York City, NY 10031

The oscillations of acoustically driven bubbles in a liquid are explored. In the strong forcing regime, where bubbles emit sonoluminescent radiation, the velocity of the bubble wall becomes comparable to the speed of sound in the gas and in the liquid. The Rayleigh - Plesset equation, which determines the motion of the bubble wall and several modifications are discussed. The results for the emitted sonoluminescent radiation turn out to be very sensitive to the motion of the bubble wall close to the minimum radius. The analysis of the sensitivity of a bubble to surface instabilities is extended to the strong forcing regime. It is found that the gas and liquid parameters strongly influence the stability regime of the bubble oscillations. These include the viscosity of the liquid as well as the surface tension of the liquid-gas interface. Detailed predictions of the dependence of the stability on these parameters is given. A qualitative explanation of some of the characteristics of the sonoluminescent radiation follows from this analysis.

INTRODUCTION

Sonoluminescence (SL), the emission of light from an oscillating gaseous bubble in liquids, has been recently carefully explored, both experimentally[1–7] and theoretically[8,9,11,10,12–18]. It has been determined that the light emitted is of very short duration (less than $50\,ps$)[2], high emitted power (more than $30\,mW$), and that the spectrum of the emitted radiation shows similarities to the black body spectrum[3].

While there is a variety of approaches to the problem of SL[12,15–17], the explanation based on the production of shock waves in the contracting gaseous bubble seems the most successful. Some of the basic features of the SL radiation have been explained, including the extremely short time scale, high energy concentration[8–11] and the main characteristics of the spectrum of the emitted radiation[8,9,18]. Yet, some of the most intriguing facts about the SL radiation have not been explained. One would like to understand why noble gas bubbles behave so differently from air bubbles[5,7]; Why is it so much easier to produce single bubble SL in water than in other liquids[1,7,19]; Why does the intensity and the spectrum of the SL radiation varies so much for different gases[5]?

The purpose of this paper is twofold. Firstly, it is to examine the applicability of the commonly used Rayleigh-Plesset (RP) equation to the problem of strongly driven oscillations of bubbles in liquids (section I). Based on this analysis, we formulate the approach (mostly based on the previous work by Crum[20] and Prosperetti et al.[21–24]), which more correctly describes bubble oscillations. The comparison with our previous results[18], which involved solving of the hydrodynamic equations for the gas in the bubble, gives further justification to this approach. The results of the RP (and similar) equations are compared with the “full” formulation based on the solution of the hydrodynamic equations for the gas in the bubble. Our main contribution here is careful analysis of the RP and similar equations in strongly forcing regime of bubble oscillations, what have not been done previously. We show that the RP equation has to be corrected in order to correctly describe the motion of the bubble wall under experimental conditions which are common in the sonoluminescent experiments. The results for the sonoluminescent radiation following from different models and for different parameters are given. Secondly, this paper serves to explore the stability of a bubble under surface deformations (section II). The formulation from section I allows to extend the previous stability analysis by Prosperetti[25] and Brenner et al.[26] to the sonoluminescent regime of bubble oscillations. We explore a part of the reach parameter space, consisting of the various liquid and gas parameters, and find that some of the answers to the above mentioned questions naturally follow from this analysis.

I. THE BUBBLE EQUATION

Considerable research about the forced oscillations of bubbles in a sound field has been performed during last 60 years. Following original work by Rayleigh[27], certain improvements were formulated by Plesset[28,29]. Furthermore, the effects of mass[7,30–33,40] and heat diffusion[20–24,29,34], compressibility of the liquid[21,35,36], and non-adiabatic behavior of the gas in the bubble (shock waves)[8,9,11,18] have been explored. Our goal here is to extend the previous analysis to the case of the bubble oscillations which are strongly driven by a sound field.

The problem is formulated in part A. The subject of the part B is the analysis of the previous work in the field and formulation of the model of the bubble oscillations which seems to be the most accurate (and still relatively simple). In B.1 we give arguments for the use of the modification of the RP equation, which is correct to the first order in $\dot{R}/c_l$, where $\dot{R}$ is the velocity of the bubble boundary (hereafter called "wall"), and c_l is the speed of sound in the liquid. In B.2 is shown that this equation is approximately correct even if shock waves are produced in the bubble. A model (based on the "polytropic" approach), which should serve as a first order approximation to the process of heat flow between the bubble and the liquid, is reevaluated in B.3. In the part C we compare the results of the various models.

A. Formulation

The Rayleigh[27] - Plesset[28,29] equation has been widely used for exploring the oscillations of spherically symmetric bubbles exposed to a sound field

$$R\ddot{R} + \frac{3}{2}\dot{R}^2 = \frac{1}{\rho_l}\left[P_g(R) - P_a(t) - P_0 - \frac{2\sigma}{R}\right] \ . \tag{1}$$

Here $R(t)$ is the time dependent bubble radius, $P_a(t)$ is the acoustic pressure amplitude, P_0 is the hydrostatic pressure, σ is the surface tension and ρ_l is the liquid density. $P_g(R)$ is the pressure in the gas, just next to the bubble wall. If one takes into account the viscosity of the liquid ν_l (kinematic) and the possibility of acoustic radiation, the following equation is obtained

$$\begin{aligned} R\ddot{R} + \frac{3}{2}\dot{R}^2 = {} & \frac{1}{\rho_l}\left[P_g(R) - P_a(t) - P_0 - \frac{2\sigma}{R}\right] \\ & + \frac{R}{\rho_l c_l}\frac{d}{dt}[P_g(R) - P_a(t)] - 4\nu_l\frac{\dot{R}}{R} \ . \end{aligned} \tag{2}$$

The term involving speed of sound in the liquid, c_l, accounts for the compressibility of the liquid. This equation has to be coupled with an equation which determines $P_g(R)$. The usual (and the simplest) approach is to assume that this pressure follows from the following relation which connects the pressure in the bubble and its radius

$$P_g = P_0 \, \frac{\left(R_0^3 - a^3\right)^\kappa}{\left(R^3 - a^3\right)^\kappa} \, , \tag{3}$$

where R_0 is the equilibrium radius of the bubble, a is the assumed hard core radius and κ is the polytropic exponent[20–22,29], which determines the thermodynamic conditions in the bubble (for the adiabatic conditions, $\kappa = \gamma$ (the ratio of specific heats for the gas), for the isothermal conditions, $\kappa = 1$). The value of κ to use will be discussed later in this section.

B. The region of applicability and possible improvements of the RP equation

The approximations made in deriving these equations are numerous and, in come cases, crude. The heat and mass flow between the bubble and the liquid have been neglected. In addition, it is tacitly assumed that the speed of the bubble wall is small compared to the other characteristic velocities in the problem, namely the speed of sound in the gas and the speed of sound in the liquid. Finally, it is assumed that there is such a thing as "bubble wall" - well defined boundary between the bubble and the liquid. Still, the RP equation, Eq. (1), and its extension, Eq. (2), have been proven[20,22,37,38] to correctly describe the oscillations of the gaseous bubbles in a sound field, especially for moderate driving pressures.

Unfortunately, since we are interested in strongly forced bubble oscillations, where the contraction phase (cf. Fig. **??**) happens so fast that there is the possibility that shock waves in the bubble are produced, and the SL pulse emitted, it is necessary to reconsider the approximations made in deriving the RP equation. It will be shown later in this section that use of Eqs. $(1, 2)$ in this regime of bubble oscillations leads to considerable errors. Our goal is to formulate a more precise model which can be used to correctly describe the bubble motion, and still to keep it solvable.

Let us discuss the major approximations made in deriving Eqs. $(1, 2)$, and possible improvements.

1. *Typical velocities in the problem*

In order for the RP equation to correctly describe the bubble motion, the speed of the bubble wall $\dot{R}$ should be small compared to the speed of sound in the liquid and in the bubble (in what follows, we assume the liquid to be water, if not specified differently). Inspection of Fig. **??** shows that this is not the case. The bubble wall speed $\dot{R}$, as a solution of Eq. (2) could easily reach values of few km/s. These values are higher than the speed of sound in both liquid and gas under standard conditions. Correspondingly, one could question the use of Eq. (2) in this regime.

With respect to the speed of sound in water, the situation is not too bad, since we are concerned with the speed of sound in the water just next to the bubble. The pressure in this region is very high during the compression part of the cycle. We use the phenomenological equation of state for water[35]

$$\frac{P_l + B}{P_\infty + B} = \left(\frac{\rho_l}{\rho_{l\infty}}\right)^n , \tag{4}$$

where the values of $B = 3049.13\,atm$ and $n = 7.15$ give very good agreement with experiment for the pressures up to $10^5\,atm$. Here P_∞, $\rho_{l\infty}$ are the undisturbed values of the pressure and density of the liquid, respectively (we use $\rho_l = \rho_{l\infty}$ in what follows). The speed of sound is readily found to be

$$c_l^2 = \frac{n(P_l + B)}{\rho_l} . \tag{5}$$

Assuming that the polytropic formula (Eq. (3)) for the pressure in the gas is correct, and knowing that the connection between the pressure in the gas and the pressure in the liquid just next to the bubble wall is given by $P_l = P_g - 2\sigma/R - 4\nu_l\rho_l\,\dot{R}/R$, one can easily verify that close to the minimum of the bubble radius (where $\mid \dot{R} \mid$ is largest), P_l reaches very high values, typically more than $10^4\,atm$. The consequence of this high pressure is that the speed of sound in the liquid is much higher than its standard value. Typical results for the speed of sound in the water next to the bubble, for high acoustic pressure amplitudes, are about $4 - 5\,km/s$. This speed is larger than the maximum speed of the bubble wall obtained by solving Eq. (2), if bubble is not driven with extremely high acoustic pressures (more than $1.5 - 1.6\,atm$). Still, since these speeds are of the same order of magnitude, one would like to use the approach where the motion of the bubble is correct at least to the first order in $\dot{R}/c_l$. This approach has been established[21,35,36]. Prosperetti[21] has actually shown that there is a whole family of equations which are correct to the first order in small quantity $\dot{R}/c_l$. We choose the following member of the family to determine the motion of the bubble (for details, see[21,35])

$$R\ddot{R}\left(1 - \frac{\dot{R}}{c_l}\right) + \frac{3}{2}\dot{R}^2\left(1 - \frac{\dot{R}}{3c_l}\right) = \frac{1}{\rho_l}\left(1 + \frac{\dot{R}}{c_l}\right)\left[P_l(R,t) - P_0 - P_a\left(t + \frac{R}{c_l}\right)\right] + \frac{R}{\rho c_l}\frac{dP_l(R,t)}{dt} , \tag{6}$$

where $P_l(R,t)$ is the pressure in the liquid just next to the bubble wall (connected with the pressure in the gas in the manner which was explained above), and $P_a(t + R/c_l)$ is the time - delayed driving pressure. This and similar equations have been successfully used to model the motion of the bubble[1,21,33,36]. The importance of the use of the speed of sound in the liquid given by Eq. (5) will be further emphasized at the end of this section.

2. *Spatial uniformity of the gas in the bubble*

One of the assumptions in deriving of the bubble equation was that the thermodynamic variables for the gas in the bubble interior do not develop any spatial structure. By comparing $\dot{R}$ with the speed of sound for the gas in the bubble, c_g, which follows from the polytropic equation, Eq. (3), one can easily see that $\dot{R} > c_g$, meaning that the formation of shock waves in the bubble could be expected. It has been shown[8,9,11,18] that this is really the case. This means that the use of Eq. (3) is not a priori justified. Here lies one of the motivations for our previous work[18], where the gas dynamic equations for the gas in the bubble has been solved. The results for the space - time profile of the pressure, velocity and temperature of the gas in the bubble are presented in Fig. **??**. The approach[18] is actually more complete in the sense that it accounts for various mechanical energy loss mechanisms in the high temperature gas, like dissociation, ionization and radiation. While it is shown[18] that the proper understanding of the energy loss mechanisms and the radiation - matter coupling is of crucial importance in explaining SL, our numerical results imply that the inclusion of these processes in the hydrodynamic equations is not significant in determining the motion of the bubble wall. Furthermore, our results[18] show that the motion of the bubble wall is not considerably disturbed by the production of a shock wave in the bubble. Of course, the reflection of the shock wave from the bubble wall (see Fig. **??**) leads to a certain disturbance of the bubble wall motion, but this effect is not significant. The conclusion is that one can rather safely use the values for P_g following from the polytropic formula in Eq. (6)[39].

3. Heat and Mass flow between the bubble and the liquid

The more complete approach to the bubble problem should definitely include the possibility of the heat and mass flow between the bubble and the liquid. This would involve solving Navier-Stokes rather than Euler equations for the gas and for the liquid simultaneously, and complicate the problem to the level where even numerical solutions would be hard to obtain. Fortunately, remarkable stability of bubble oscillations, which could last for hours, and also the stability of the SL emission[2], seem to imply that the net heat and mass flow vanish during one period (acoustic cycle). One could use this periodicity to simplify the problem.

The mass flow between the bubble and the liquid has been extensively explored, both experimentally and theoretically[7,30–33,40]. It has been shown that the mass flow is important in order to determine the equilibrium bubble radius, R_0. While the diffusion equation seems to work fairly well in the weak forcing regime (where the bubble does not produce the SL pulse), a mysterious additional mass flow occurs in the SL regime[7]. It is feasible that the shock waves produced in the bubble might be the source of this effect. Until this problem is solved, we have to use R_0 as a (experimentally measurable) parameter in the problem.

The heat flow has been carefully explored as well[20–24,29,33,34]. The common approach has been to introduce effective "polytropic exponent" κ in place of the ratio of specific heats γ (as it has already been done in Eq. (3)). This polytropic exponent should effectively account for all of the heat exchange processes between the bubble and the liquid. The agreement between the theory and the experiment is fairly good and the conclusion is that the bubbles whose equilibrium radius is much less than its resonant radius, (this is the case in the SL experiments), behave almost isothermally ($\kappa \approx 1$)[20]. Unfortunately, the experimental support is missing in the SL regime.

Still, by examining effect qualitatively, one can arrive at certain conclusions. The time scale T_s connected with the thermal diffusion in gas is given by $T_s \sim L^2/D$, where L is the typical length scale and D is the coefficient of thermal diffusion (for air $D \approx 0.2\,cm^2/s$). For a typical bubble size of about $10\,\mu m$, this gives $T_s \sim 5\,\mu s$, shorter than typical acoustic period $T_a \sim 30\,\mu s$. This means that the heat conduction might be important in the problem. On the other hand, the contraction part of the cycle, especially when the temperature of the gas is very high, is very short, $\sim 0.1\,\mu s$. Following these arguments, one is tempted to conclude that the bubble oscillations could be modeled as the isothermal expansion (up to the maximum radius), followed by the adiabatic compression (a similar approach has already been used[33]). This model is necessarily incomplete, since it would result in a net heat flow from the liquid to the bubble during one acoustic cycle. We assume that the temperatures of the bubble and the liquid are going to equilibrate during the long period after the first minimum of the bubble radius, when the bubble is slowly oscillating around its equilibrium radius, waiting for the next rarefaction phase of the acoustic wave. Since we are mostly interested in the processes which determine a bubbles collapse, and its behavior around its minimum radius (during which the SL pulse is emitted), we do not consider this equilibration process in more details. So, in order to account for the heat exchange between the bubble and the liquid during the slow expansion from the equilibrium to the maximum bubble radius, we model our "polytropic exponent" in the following way

$$\kappa = \begin{cases} 1 & if\ t\ <\ t_{max} \\ \gamma & if\ t\ >\ t_{max} \end{cases} , \tag{7}$$

where t_{max} is defined by $R(t_{max}) = R_{max}$, and γ is determined by the gas in the bubble.

C. Comparison of the various models and sonoluminescent radiation

Finally, let us summarize our results of this section. In Fig. ?? we show the numerical and experimental results for the radius versus time for an air bubble in water, exposed to the sound field. We see that the agreement between the theory and the experiment is fairly good. If the polytropic exponent κ is assumed to be equal to 1 during the expansion, the bubble expands (and compresses) more than in the adiabatic case. Still, the experimental data[4] are not precise enough to verify which value of κ is the best.

The most important part of this figure is the inset, which shows the bubble wall motion close to the minimum radius. We have already seen (cf. Fig. ??, the solution of Eq. (2)), that the bubble wall velocity is comparable to the speed of sound in the liquid next to the bubble, which is about $4\,km/s$ for our choice of parameters. The inset in Fig. ?? shows that there is a considerable change in the results if Eq. (6), correct to the first order in $\dot{R}/c_l$, is used (compare the full line (RT) and the broken (v/c) line in Fig. ??). The bubble boundary moves much slower if this, more realistic, formulation is used. The change of the polytropic exponent κ, in the manner explained above, does not lead to significant differences close to the bubble minimum (compare the broken (v/c) line and the dotted (κ) line in Fig. ??).

The conclusion is that it is important to include the corrections to the original RP formulation, if the precise results for the motion of the bubble wall close to the minimum radius are desired. In the next section, we will see that it is necessary to have precise results for the bubble motion during this period, since they influence the stability of the bubble oscillations.

Before proceeding to the stability analysis, let us see what is the influence of the various models presented in this section on the sonoluminescent radiation. The results for the average power emitted in the optical region are given in Table I. For later reference, the results for different values of the surface tension and the liquid viscosity are given as well. The duration of the SL pulse for different models and parameters does not seem to vary considerably, being typically about $10\,ps$. Important observations to be made are as follows:

- First part of the table clearly shows that the SL pulse is extremely sensitive to the motion of the bubble wall. There is an order of magnitude decrease in the SL emission if Eq. (6) is used, compared to Rayleigh-Plesset equation. We would also like to emphasize that, if the standard value of the c_l is used in Eq. (6), the motion of the bubble wall close to the minimum radius will be slower than the local speed of sound in the gas, preventing shock wave from being produced.
- The difference between the second $(c_l\,(\infty))$ and the third column $(c_l$ (RP)) of the first part of the table shows the influence of the acoustic radiation term, which is present in Eq. (2), but effectively absent if $c_l \to \infty$ limit is taken in Eq. (6) (the small kinematic term $4\nu_l\rho_l\dot{R}/R$ is not influential). Clearly, the acoustic radiation leads to weaker collapse (and rebound) of the bubble, and to less SL radiation. This effect is more important for lower acoustic pressures, at least concerning the initial conditions for the shock production and SL radiation.

- Second part of the table has to do with polytropic exponent κ and might look surprising at first. The results say that if the gas gains energy from the liquid during the expansion part of the cycle (through heat conduction), less SL radiation is emitted. The way to understand this fact is as follows: If the expansion of the bubble is almost isothermal, the change in the pressure during this part of the cycle will be smaller (compared to the adiabatic expansion). Correspondingly, during the compression phase, the pressure in the bubble will build up much higher, preventing bubble from collapsing as fast as it would if the pressure at the maximum radius was smaller. That leads to the production of weaker shock wave, lower temperatures, and less SL radiation.
- Last two parts of the table give the results for a few values of the surface tension and liquid viscosity. The results could be easily understood (at least in qualitative manner). Higher liquid viscosity slows down the bubble collapse, and the produced shock wave is weaker. Higher viscosity value effectively raises the threshold acoustic pressure needed to produce sonoluminescence. Similarly, if the surface tension is decreased, the bubble expands more and the collapse is stronger. The role of surface tension, especially close to the minimum radius is not clear, and we will discuss it more in the following section.

II. STABILITY OF THE BUBBLE OSCILLATIONS

In this section we explore the stability of the bubbles with respect to nonspherical surface deformations. Based on the section I, we are able to extend the results by other researchers in the field to the SL regime of the bubble motion (part A). Furthermore, the analysis of the stability of a bubble for various experimental conditions is given (part B). This is the most important contribution of this paper. It is shown that qualitatively different behavior of bubbles in various liquids and with various gas content can be understood based on this analysis.

A. Formulation of the problem

One could expect two instability mechanisms to take place during bubble oscillations. The first is the typical Rayleigh-Taylor instability[41], occurring whenever less dense fluid (gas) is accelerating into more dense fluid (liquid). The second mechanism is parametric instability, resulting from the accumulation of nonspherical perturbations over many periods. Some experimental support for the onset of surface instabilities is given in[25,42].

The problem of the time evolution of the distortion of the spherical surface, given by $R(t) + \epsilon\, a_{nm}(t)\, Y_n^m(\theta, \phi)$, for the incompressible liquid, was formulated by Plesset[43] and further developed[21,25,34,42,44–46]. Here ϵ is a small parameter and future analysis is valid to the first order in ϵ; $Y_n^m(\theta,\phi)$ is a spherical harmonic of degree $n \geq 2$. The basis of our approach is Eq. (6), valid to the first order in the small quantity $\dot{R}/c_l$. Consistency requires keeping only the first order terms in either of these two small parameters (ϵ, $\dot{R}/c_l$). To this order of approximation, our equations for the amplitude $a_{nm}(t)$ coincide with those given by Brenner et al.[26]. [It has been shown[25] that $a_{nm}(t)$ is independent of index m which is correspondingly omitted in the rest of this paper.]

$$\ddot{a}_n + B_n(t)\dot{a}_n + A_n(t)a_n = 0 \ , \tag{8}$$

where

$$B_n(t) = 3\frac{\dot{R}}{R} + \left[(n+2)(2n+1) - 2n(n+2)^2\frac{\delta}{R}\right]\frac{2\nu_l}{R^2} \ , \tag{9}$$

$$\begin{aligned} A_n(t) = &-(n-1)\frac{\ddot{R}}{R} + (n^2-1)(n+2)\frac{\sigma}{\rho_l R^3} \\ &+ \left[(n-1)(n+2) + 2n(n+2)(n-1)\frac{\delta}{R}\right]\frac{2\nu_l\dot{R}}{R^3} \ . \end{aligned} \tag{10}$$

These equations are valid to the first order in small quantities ϵ, $\dot{R}/c_l$ and the viscous-diffusion length δ, given by $\delta = min\left[\sqrt{\nu_l/\omega}, R/2n\right]$[26]. The time dependent bubble radius R, as well as the velocity $\dot{R}$ and the acceleration $\ddot{R}$, are determined by solving Eq. (6). Polytropic exponent κ follows from Eq. (7), and the pressure in the gas P_g from Eq. (3).

The analysis of parametric instability based on Eqs. (8-10) is given in[26], where the weak forcing limit was explored as well, showing that Eq. (8) reduces to Mathieu's equation. This observation allows to more easily understand the modulated oscillations in P_a/R_0 diagram in Fig. **??**. It is found that only low modes (small n) are important in determining parametric stability. The results given in Fig. **??** and following figures are the superposition of the first five modes.

The Rayleigh - Taylor (RT) instability occurs during extremely high positive acceleration of the bubble into the liquid, around the time when the bubble reaches its minimum radius. WKB type analysis of Eq. (8), using $a_n(t) \sim \exp(S_n(t)$, gives the following expression for the average amplification $\bar{S}_n$

$$\bar{S}_n \sim \int \left(-\frac{B_n}{2} \pm \sqrt{\frac{B_n^2}{4} - A_n}\right) dt \ . \tag{11}$$

The integral is calculated over the time period during which the bubble is accelerating in the liquid ($\ddot{R} > 0$). The criterion for establishing the RT (in)stability is to verify if the amplification given by Eq. (11) could produce the growth of molecular fluctuations to the size of the bubble. The diagram of the RT stability is shown in Fig. ??. With the respect to the RT type instability, the bubble is stable in the part of the parameter space which is to the left of the RT line in Fig. ??[47]. The bubble is sensitive to the RT type instability just for the very short time of about $1\,ns$, when it is close to its minimum radius, during which bubble wall accelerates into the liquid with $\ddot{R} \approx 10^{12} - 10^{13}\,m/s^2$. No instability has been observed for the initial expanding part of the bubble cycle. Our results are similar to those given by Brenner et al.[26]. Differences arise from the fact that we use Eq. (6) for determining spherically symmetric part of the bubble motion, compared to use of Eq. (2)[26]. We noticed that modulated oscillations for parametric stability are greatly suppressed by using Eq. (6) instead of Eq. (2).

One can understand the stability diagram in Fig. ?? in the following way. Parametric instability is the "slow" one. It builds up through many acoustic cycles. So, if a bubble reaches the unstable region (for example, if acoustic pressure amplitude is slowly turned on), it will change its equilibrium radius through the process of mass diffusion (or some other mass - exchange process). The "islands" of parametric stability visible in Fig. ?? still have to be observed experimentally.

The Rayleigh - Taylor instability, on the other hand, acts extremely quickly and destroys the bubble, eventually by breaking it into microbubbles. Still, in Fig. ??, we can see that for most of the experimental parameters (R_0 and P_a), the bubble first comes into the regime of parametric instability, what makes it changing its equilibrium radius R_0, correspondingly avoiding reaching the threshold for the RT instability.

Influence of non-spherically symmetric instabilities on SL can easily be understood. Any asymmetry in the bubble shape will disturb the initial conditions for the production of shock waves in the bubble. Since the time - evolution of shock waves is highly sensitive to the initial conditions, the converging phase of the shock propagation will be disturbed as well, (spherical symmetry is not satisfied any more), and, correspondingly, one does not expect strong energy focusing, required for the production of the SL pulse.

In order to better understand the importance of the stability effects on the bubble dynamics and the SL emission, we explore the changes in the stability diagram (Fig. ??) for various experimental parameters.

B. Analysis

Here we analyze the influence which some of the physical parameters could have on the stability results. Before we proceed, let us explain the motivation for this project. It was shown[18] that the SL emission is extremely sensitive on even slight changes of the experimental parameters, like the equilibrium bubble radius or the acoustic pressure amplitude. Experimentally it is known[5] that big differences in the strength and characteristics (e.g. spectrum) of the SL radiation occur for different gases. Finally, single bubble SL is so much more stable and easier to obtain in water than in other liquids[19]. On the other hand, multiple bubble SL, most probably based on transient cavitation[14,48–51], has been observed for decades in various liquids. We would like to explore the possibility that some of these observations could follow from the fact that the bubble could be under different stability regimes if some of the experimental parameters are changed. The simplest example is the strong dependence of both parametric and the RT instability thresholds on the equilibrium bubble radius R_0 (cf. Fig **??**). The equilibrium radius R_0 is determined by the nature and concentration of dissolved gases[5,7]. So, one can easily understand why bubbles, whose gaseous content varies, will behave differently, even if all other experimental conditions are the same.

In what follows, we concentrate on the influence of the viscosity of the liquid ν_l, the surface tension σ and the ratio of specific heats of the gas, γ. The results for different γ could apply to different gases solvated in liquids. The viscosity and surface tension results apply to different liquids, but they might also have importance for the case of SL in water. Namely, it is interesting to note that the best correspondence between the experimental results for the bubble radius versus time and the RP equation was obtained with rather unusual values for the (kinematic) viscosity and the surface tension[4,33,40]. Of course, these values were used only as fitting parameters[52]. [Here one could also think of the possibility of contamination of the water[53].] The surface tension and viscosity entering Eqs. $(1, 2, 6)$ might as well be considered as effective parameters, which include other effects, neglected in deriving the RP equation. Different experimental conditions, e.g. the nature or the concentration of the dissolved gas, or the liquid temperature[31], could change these effective parameters and correspondingly change the regime of bubble oscillations. The surface tension, in particular, could be influenced by the temperature in the bubble (both viscosity and surface tension of water, for example, are decreasing functions of temperature[54]). Finally, the experimental fact that the bubbles (for example air bubbles) *are* stable for the values of R_0, P_a for which one would expect them to be unstable based on the stability analysis (cf. Fig. **??**), seems to imply that the effective values of the surface tension and viscosity might be different than standards ones. [The fit of the experimental data[4] to the RP equation was made with value of the viscosity of $0.07\, cm^2/s$. For this value of "effective" viscosity, the complete region of the parameter space shown in Fig. **??** will be stable (see also Fig. **??**).]

The stability diagram in the 3D parameter space, consisting of the acoustic pressure amplitude P_a, the equilibrium bubble radius R_0, and the viscosity of the liquid ν_l is shown in Fig. **??**. The front plane of this figure (for $\nu_l = 0.01\,cm^2/s$) was previously shown (more precisely) in Fig. ??. One can easily see that parametric stability is very sensitive to the changes of viscosity. As viscosity is increased, the bubble becomes more stable with respect to parametric instabilities (i.e., for fixed R_0 the bubble is stable for higher acoustic pressure amplitudes). Yet, the RT stability (the region below the RT surface in Fig. ??) does not change so much, thus at some point the threshold for launching the RT instability is reached while the bubble is still in a parametrically stable regime. Correspondingly, the bubbles in more viscous fluids might be expected to be unstable with respect to the RT instability.

The situation is different if we consider the changes of surface tension. This is illustrated in Fig. ??. Here we see that both parametric and the RT thresholds rise with the increase of surface tension. This is what one would expect, since it is well known[25] that surface tension plays an important role in stabilizing bubble oscillations. We would like to bring readers attention at this point to the use of "effective" surface tension of less than a half of its standard value for water ($72.5\,dyn/cm$)[33]. We suggest careful experimental examination of these "effective" parameters for different gases dissolved in liquids. If these values of effective parameters (surface tension or viscosity) are varying, one could eventually understand the different behavior of bubbles with different gaseous content. Another interesting observation is that the surface tension of water is high compared to other common liquids (e.g. for ethanol $\sigma = 21.97\,dyn/cm$, for ethylene glycol $\sigma = 24.06\,dyn/cm$, for acetone $\sigma = 23.46\,dyn/cm$, for 1-butanol $\sigma = 24.93\,dyn/$, for 1-pentanol $\sigma = 25.36\,dyn/cm$; all values are at $25°C$[54]). This means that bubble oscillations will be much more stable in water, compared to the above mentioned liquids. Perhaps here we have the answer to the question why bubble oscillation are unstable in some of these liquids[19]. On the other hand, for mercury, $\sigma = 485\,dyn/cm$[54], so one would expect cavitation to be very stable there (of course, if it is possible because of other effects).

The next graph, Fig. ??, is for various γ's (effectively, for different gaseous bubble content). Recalling our previous discussion about the effective γ (polytropic exponent κ), the change of it might effectively account for various physical processes not included in our formulation of the bubble equation, like heat conduction, damping, etc. The thresholds for both parametric and the RT instability are not very sensitive to the change of κ, but one can still notice opposite trends, especially for small bubbles ($R_0 \approx 3-4\,\mu m$). While the RT threshold is increasing with the increase of κ, the parametric threshold is decreasing. For small κ, the threshold for the RT instability is lower than the upper limit for parametric stability, implying that for these values of the effective polytropic exponent, bubbles might be very unstable for the acoustic pressure amplitudes and the equilibrium bubble radii typically used in the SL experiments. The increased stability of the noble gas bubbles, observed experimentally[5], may result from this effect.

At this point is hard to make precise predictions about the stability of bubbles for particular liquid/gas combination, since the change of either gas or liquid produces change of many parameters, not only one. Still, certain experimental data, e.g. the instability of the bubbles with polymolecular gases, or the instability of air bubbles in the nonaquas liquids with low surface tension, could easily be understood.

CONCLUSION

The main objective of this paper is to show that the stability analysis of the bubbles undergoing forced oscillations in a sound field leads to better understanding of the influence of various experimental parameters on the nature of the bubble oscillations in the strongly forcing regime. We show that variation of the gases and liquids used in SL experiments could lead to the dramatic changes in stability of the bubbles and the SL radiation. Water seems to be a convenient medium for SL experiments because of its high value of surface tension. Possibly, following this approach, one can also understand other interesting experimental observations (like the sudden change of the size of air bubbles[5], or the instability of pure nitrogen bubbles[5]). Furthermore, the sonoluminescent radiation, being highly nonlinear effect resulting from the production of shock wave(s) in a bubble, is itself very sensitive to the manner in which bubble oscillates. For example, a few percent change of the equilibrium bubble size, which might result from parametric instability, would lead to an order of magnitude difference in the resulting SL radiation[6,18].

We have also presented considerable improvements which should be used for the numerical calculations of the spherically symmetric part of bubble oscillations. These improvements are important when it comes to the strongly nonlinear phenomena, such as the production of shock waves, which are very sensitive to the initial conditions.

Clearly, the answers which are given here are of a qualitative nature. Future research, both experimental and theoretical is required in order to gain further insight into the exciting phenomena of sonoluminescence and bubble stability.

ACKNOWLEDGMENTS

We thank Joel Koplik and Michael Shelley for reading the manuscript and for providing us with the useful comments. We are especially grateful to Andreas Acrivos and Chi Yuan for valuable suggestions.

* E-mail: kondic@cims.nyu.edu

[1] D.F. Gaitan, L.A. Crum, C.C. Church and R.A. Roy, "Sonoluminescence and bubble dynamics for a single, stable, cavitation bubble," J. Acoust. Soc. Am. **91**, 3166 (1992).

[2] B.P. Barber and S.J. Putterman, "Observation of synchronous picosecond sonoluminescence," Nature, **352**, 318 (1991).

[3] R. Hiller, S.J. Putterman and B.P. Barber, "Spectrum of synchronous picosecond sonoluminescence," Phys. Rev. Lett. **69**, 1182 (1992).

[4] B.P. Barber and S.J. Putterman, "Light scattering measurements of the repetitive supersonic implosion of a sonoluminescing bubble," Phys. Rev. Lett. **69**, 3839 (1992).

[5] R. Hiller, K. Weninger, S.J. Putterman and B.P. Barber, "Effect of noble gas doping in single-bubble sonoluminescence," Science **266**, 248 (1994).

[6] B.P. Barber, C.C. Wu, R. Löfstedt, P.H. Roberts and S.J. Putterman, "Sensitivity of sonoluminescence to experimental parameters," Phys. Rev. Lett. **72**, 1380 (1994).

[7] B.P. Barber, K. Weninger, R. Löfstedt and S.J. Putterman, "Observation of a new phase of sonoluminescence at low partial pressures," Phys. Rev. Lett. **74**, 5276 (1995).

[8] C.C. Wu and P.H. Roberts, "Shock-wave propagation in a sonoluminescing gas bubble," Phys. Rev. Lett. **70**, 3424 (1992).

[9] C.C. Wu and P.H. Roberts, "A model of sonoluminescence," Proc. Roy. Soc. (London), **445**, 323 (1994).

[10] H.P. Greenspan and A. Nadim, "On sonoluminescence of an oscillating gas bubble," Phys. Fluids **A5**, 3424 (1993).

[11] W.C. Moss, D.B. Clark, J.W. White and D.A. Young, "Hydrodynamic simulations of bubble collapse and picosecond sonoluminescence," Phys. Fluids **6**, 2979 (1994).

[12] V. Kammath, A. Prosperetti and F.N. Egolfopoulos, "A theoretical study of sonoluminescence," J. Acoust. Soc. Am. **94**, 248 (1993).

[13] L.A. Crum, "Sonoluminescence," Phys. Today, 22 (September 1994).

[14] L.A.Crum, "Sonoluminescence, sonochemistry, and sonophysics," J. Acoust. Soc. Am. **95**, 559 (1994).

[15] L. Frommhold and A.A. Atchley, "Is sonoluminescence due to collision-induced emission," Phys. Rev. Lett. **73**, 2883 (1994).

[16] J. Schwinger, "Casimir energy for dielectrics," Proc. Natl. Acad. Sci. USA, **89**, 4091 (1992).

[17] J. Schwinger, "Casimir energy for dielectrics: Spherical geometry," Proc. Natl. Acad. Sci. USA, **89**, 11118 (1992).

[18] L. Kondić, J.I. Gersten, C. Yuan, "Theoretical studies of sonoluminescence radiation: Radiative transfer and parametric dependence," Phys. Rev. E **52**, 4976 (1995). (to appear in Phys. Rev. E).

[19] K. Weninger, R. Hiller, B.P. Barber, D. Lacoste and S.J. Putterman, "Sonoluminescence from single bubbles in non-aqueous liquids: New parameter space for sonochemistry," preprint, (1995).

[20] L.A. Crum, "The polytropic exponent of gas contained within air bubbles pulsating in a liquid," J. Acoust. Soc. Am. **73**, 116 (1983).

[21] A. Prosperetti, "Bubble phenomena in sound fields: part one," Ultrasonics, 69, (March 1984).

[22] A. Prosperetti, L.A. Crum and K.W. Commander, "Nonlinear bubble dynamics," J. Acoust. Soc. Am. **83**, 502 (1988).

[23] A. Prosperetti, "The thermal behavior of oscillating gas bubbles", J. Fluid. Mech. **222**, 587 (1991).

[24] V. Kammath, H.N. Oguz and A. Prosperetti, "Bubble oscillations in the nearly adiabatic limit", J. Acoust. Soc. Am. **92**, 2016 (1992).

[25] A. Prosperetti, "Viscous effects on perturbed spherical flows", Quart. Appl. Math. **34**, 339 (1977).

[26] M. Brenner, D. Lohse and T.F. Dupont, "Bubble shape oscillations and the onset of sonoluminescence," Phys. Rev. Lett. **75**, 954 (1995).

[27] Lord Rayleigh, "On the pressure developed in a liquid on the collapse of a spherical cavity," Phil.Mag. **34**, 94 (1917).

[28] M.S. Plesset and S.A. Zwick, "A nonsteady heat diffusion problem with spherical symmetry," J. Appl. Phys. **23**, 95 (1951).

[29] M.S. Plesset and D.Y. Hsieh, "Theory of gas bubble dynamics in oscillating pressure fields," Phys. Fluids **3**, 882 (1960).

[30] A. Eller and H.G. Flynn, "Rectified diffusion during nonlinear pulsations of cavitation bubbles," J. Acoust. Soc. Am. **37**, 493 (1964).

[31] K.S. Suslick (editor), *Ultrasound* (VCH Publishers, New York, 1988).

[32] L.A. Crum, "Rectified diffusion," Ultrasonics, 215 (September 1984).

[33] R. Löfstedt, B.P. Barber and S.J. Putterman, "Toward a hydrodynamic theory of sonoluminescence," Phys. Fluids **5**, 2911 (1993).

[34] M.S. Plesset and A. Prosperetti, "Bubble dynamics and cavitation," Ann. Rev. Fluid Mech. **9**, 145 (1977).

[35] A. Prosperetti and A. Lezzi, "Bubble dynamics in a compressible liquid. Part 1. First-order theory," J. Fluid. Mech. **168**, 457 (1986).

[36] H.G. Flynn, "Cavitation dynamics. I. A mathematical formulation," J. Acoust. Soc. Am. **57**, 1379 (1975).

[37] W. Lauterborn, "Numerical investigation of nonlinear oscillations of gas bubbles in liquids," J. Acoust. Soc. Am. **59**, 283 (1976).

[38] L.A. Crum and A. Prosperetti, "Nonlinear oscillations of gas bubbles in liquids: An interpretation of some experimental results," J. Acoust. Soc. Am. **73**, 121 (1983).

[39] This point requires clarification. Use of the polytropic values for the pressure in the gas is acceptable if the goal is to compare the velocities of the bubble wall for various experimental conditions, like we will do in the following section. At the same time, one *should not* use these values of the pressure in the gas for the purpose of exploring of the shock waves in the bubble, since the propagation of the shock waves is very sensitive to the initial and boundary conditions. The self - consistent value, following from the hydrodynamic equations for the gas in the bubble, should be used for this purpose[18]. Finally, the extremely high temperature which develops close to the bubble center is responsible for the SL radiation, which could not be explained based on the polytropic approach.

[40] R. Löfstedt, K. Weninger, S.J. Putterman and B.P. Barber, "Sonoluminescing bubble and mass diffusion," Phys. Rev. E **51**, 4400 (1995).

[41] G. Taylor, "The instability of liquid surfaces when accelerated in a direction perpendicular to their planes. I," Proc. Roy. Soc. (London), **A201**, 192 (1950).

[42] A.I. Eller, L.A. Crum, "Instability of the motion of a pulsating bubble in s sound field," J. Acoust. Soc. Am. **47**, 762 (1970).

[43] M.S. Plesset, "On the stability of fluid flows with spherical symmetry," J. Appl. Phys. **25**, 96 (1953).

[44] G. Birkhoff, "Note on Taylor Instability," Quart. Appl. Math. **12**, 306 (1954).

[45] R.B. Chapman and M.S. Plesset, "Nonlinear effects in the collapse of a nearly spherical cavity in a liquid," J. Basic Eng. **94**, 142 (1972).

[46] H.W. Strube, "Numerische Untersuchungen zur Stabilitat nichtsphärich schwingender Blasen," Acustica **25**, 289 (1971).

[47] Similarly to the case of parametric stability, the first five modes of nonsphericall oscillations are included in the calculations. We noticed that the lowest mode ($n = 2$) is usually the one responsible for the RT instability.

[48] K.S. Suslick, "Sonochemistry," Science **247**, 1439 (1990).

[49] C. Seghal, R.G. Sutherland and R.E. Verall, "Optical spectra of sonoluminescence from transient and stable cavitation in water saturated with various gases," J. Phys. Chem. **84**, 388 (1980).

[50] C. Seghal, R.G. Sutherland and R.E. Verall, "Sonoluminescence of $NO-$ and NO_2-saturated water as a probe of acoustic cavitation," J. Phys. Chem. **84**, 396 (1980).

[51] C. Seghal, R.G. Sutherland and R.E. Verall, "Sonoluminescence intensity as a function of bulk solution temperature," J. Phys. Chem. **84**, 525 (1980).
[52] S. J. Putterman: private communication.
[53] "Real" viscosity of the water could be easily verified experimentally, following the Stokes law for the drag on a rigid sphere.
[54] *Handbook for Chemistry and Physics*, 72nd ed. (M.I.T. Press, Cambridge, 1991-1992).

Figure 1. The radius and the velocity of an air bubble for one acoustic period, resulting from Eq. (2), assuming adiabatic conditions in the bubble ($\kappa = 1.4$). These are results for an acoustic pressure of $1.325\,atm$ and an initial bubble radius of $4.5\,\mu m$. The other parameters entering are acoustic frequency $f_a = 26.5\,kHz$, $R_0/a = 8.5$, $\rho_l = 1.0\ g/cm^3$, $c_l = 1.481\,km/s$, $\sigma = 72.5\,dyn/cm$, and $\nu_l = 0.01\,cm^2/s$ (for water at 20°C). These parameters are used throughout this paper, unless specified differently. The inset is the expansion of the square close to the first minimum of bubble radius.

Figure 2. Space - time profile of the velocity, pressure and temperature of the gas (air) in the bubble. Time $t = 0$ is defined as the time when the bubble wall velocity changes sign (bubble reaches its minimum radius) and r is the distance from the bubble center. The propagation of two shock waves can easily be followed. The mechanical energy loss mechanisms mentioned in the text were not included. Note extremely high temperatures and pressures close to the bubble center.

Figure 3. Bubble radius versus time for the modified RP equation, Eq. (2) ($\kappa = 1.4$) (RP-full line), Eq. (6) ($\kappa = 1.4$) (v/c-broken line), and for the latter equation with κ following from Eq. (7) (κ-dotted line). The results for the bubble radius close to the minimum (inset) are shifted in time relative to each other. The parameters are the same as before.

Figure 4. Stability diagram of the bubble. In the part of the parameter space which is covered by the black circles, bubble is stable with the respect to parametric instability. The RT line is the boundary between the RT stable region (to the left) and the RT unstable region (to the right). All the parameters entering are the same as before. Here and in the following figures, the polytropic exponent κ is determined by Eq. (7).

Figure 5. Stability diagram for various equilibrium bubble radii R_0, acoustic pressure amplitudes P_a and liquid viscosities ν_l. In the part of the parameter space filled by the boxes, the bubble is stable with respect to parametric instabilities. The RT surface is the boundary between the part of the space where the bubble is stable with respect to the RT instability (below) and unstable (above). The other parameters are the same as before.

Figure 6. Stability diagram for various equilibrium bubble radii R_0, acoustic pressures P_a and surface tensions σ.

Figure 7. Stability diagram for various equilibrium bubble radii R_0, acoustic pressures P_a and polytropic exponents κ.

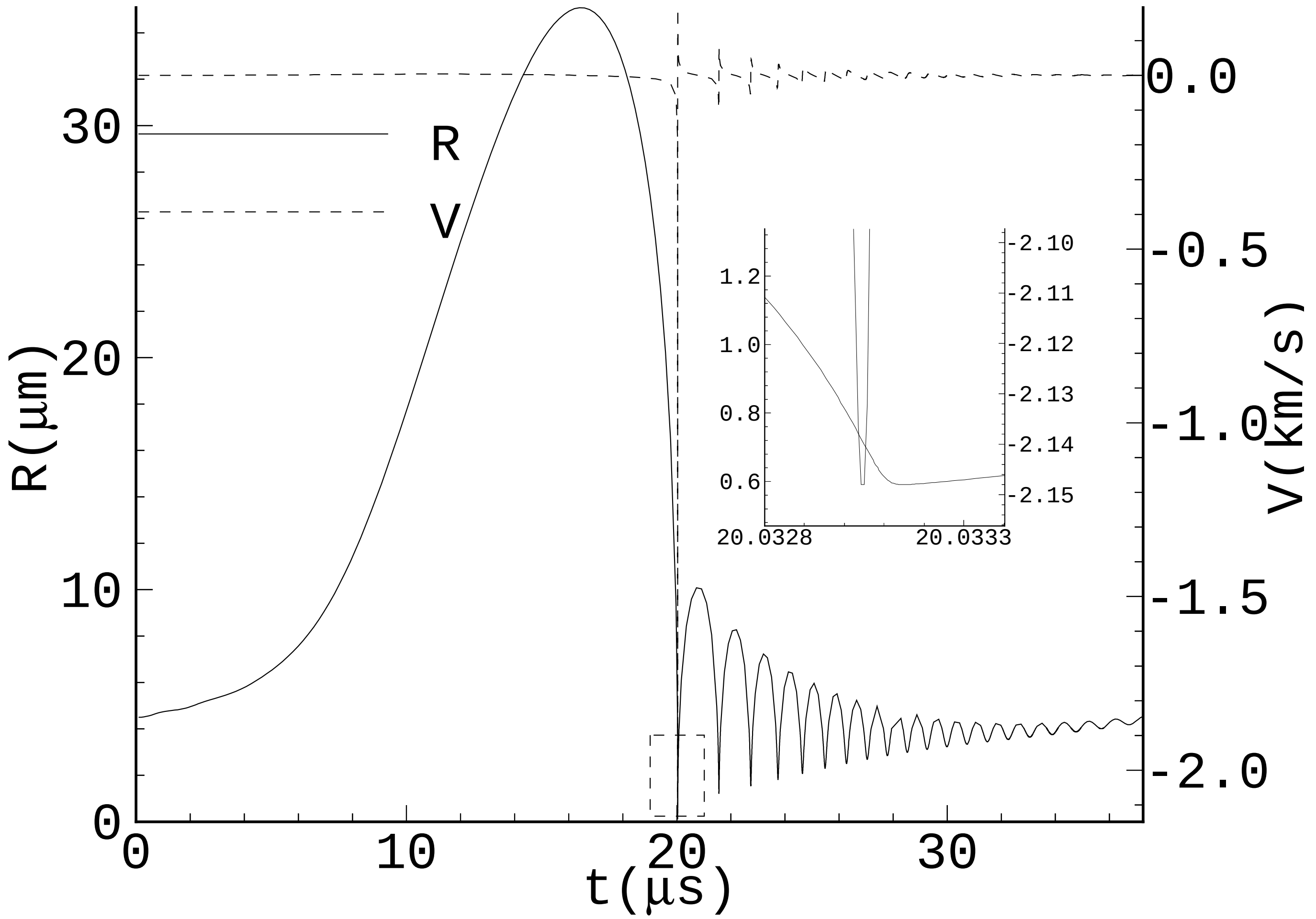
R
V
R(μm)
V(km/s)
t(μs)
0
10
20
30
0.0
-0.5
-1.0
-1.5
-2.0
1.2
1.0
0.8
0.6
-2.10
-2.11
-2.12
-2.13
-2.14
-2.15
20.0328
20.0333

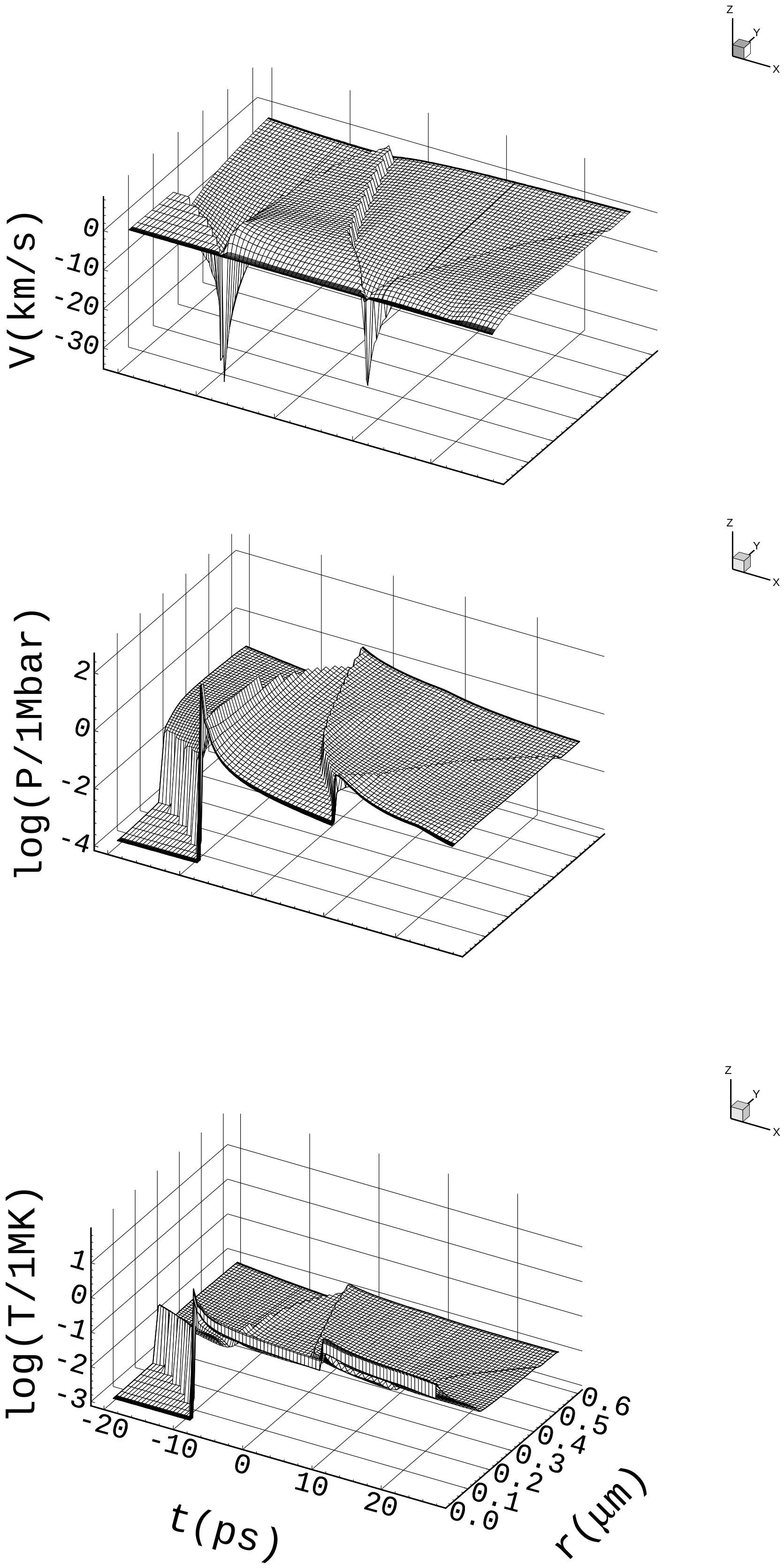

V(km/s)
0
-10
-20
-30
log(P/1Mbar)
2
0
-2
-4
log(T/1MK)
1
0
-1
-2
-3
-20
-10
0
10
20
t(ps)
0.0
0.1
0.2
0.3
0.4
0.5
0.6
r(μm)

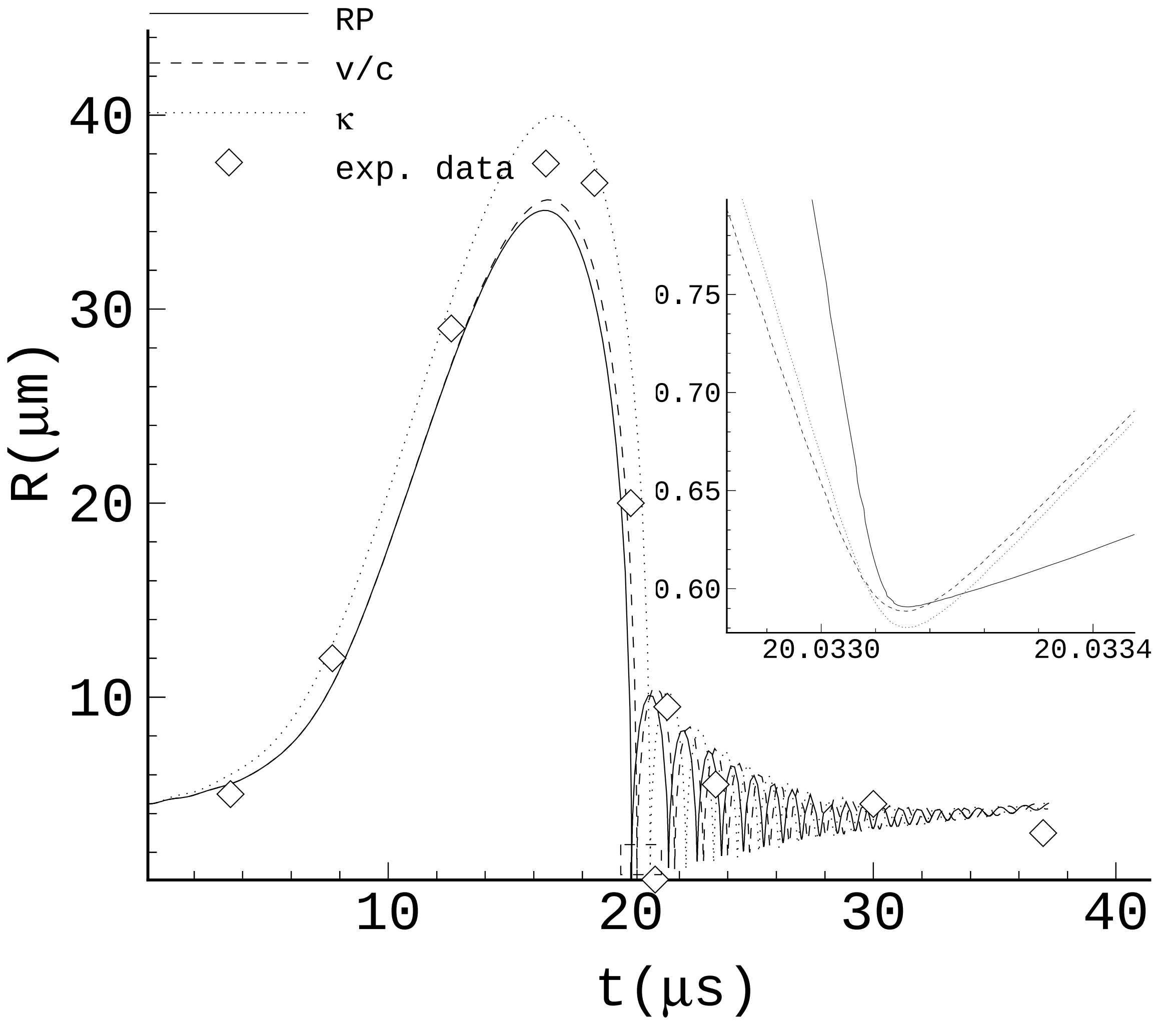
RP
v/c
κ
exp. data
R(μm)
40
30
20
10
t(μs)
10
20
30
40
0.75
0.70
0.65
0.60
20.0330
20.0334

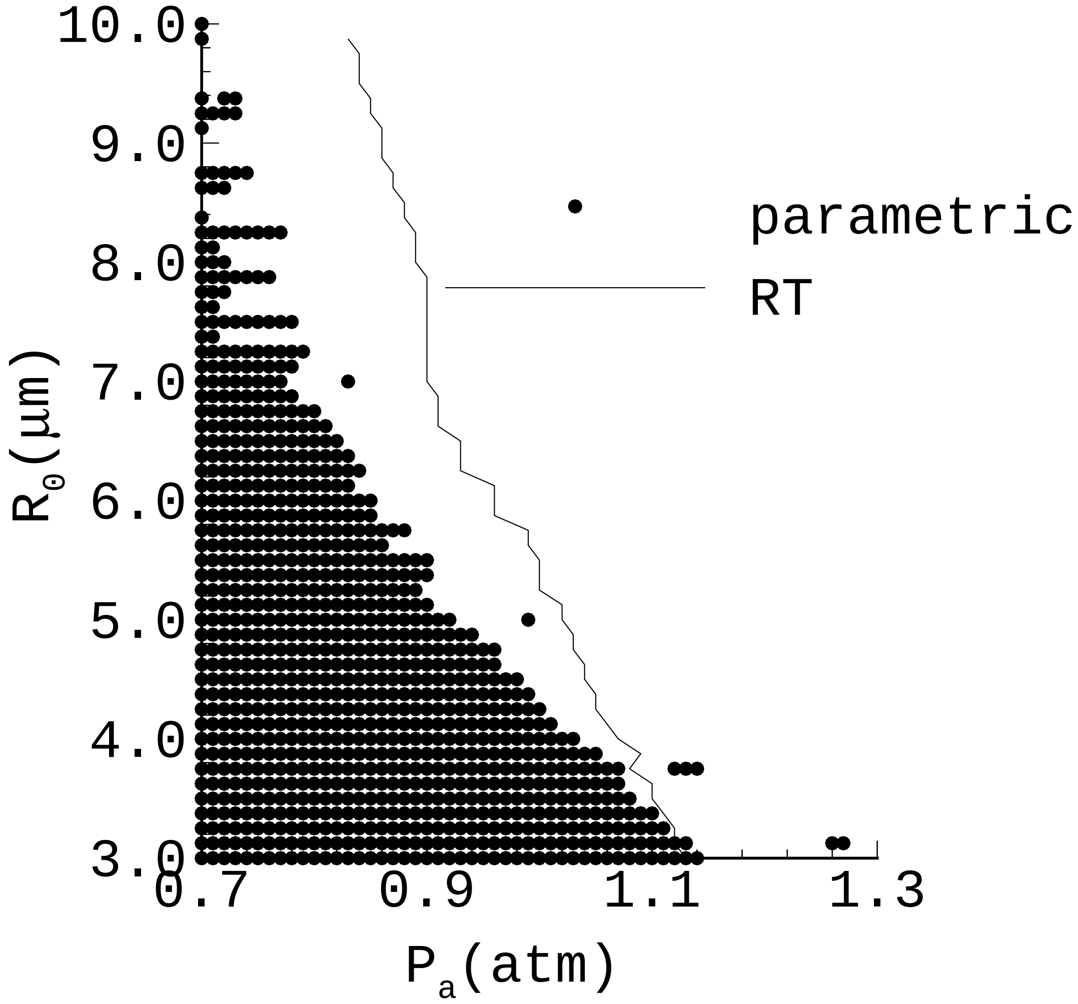

10.0
9.0
8.0
7.0
6.0
5.0
4.0
3.0
0.7
0.9
1.1
1.3
$R_0(\mu m)$
$P_a(atm)$
parametric
RT

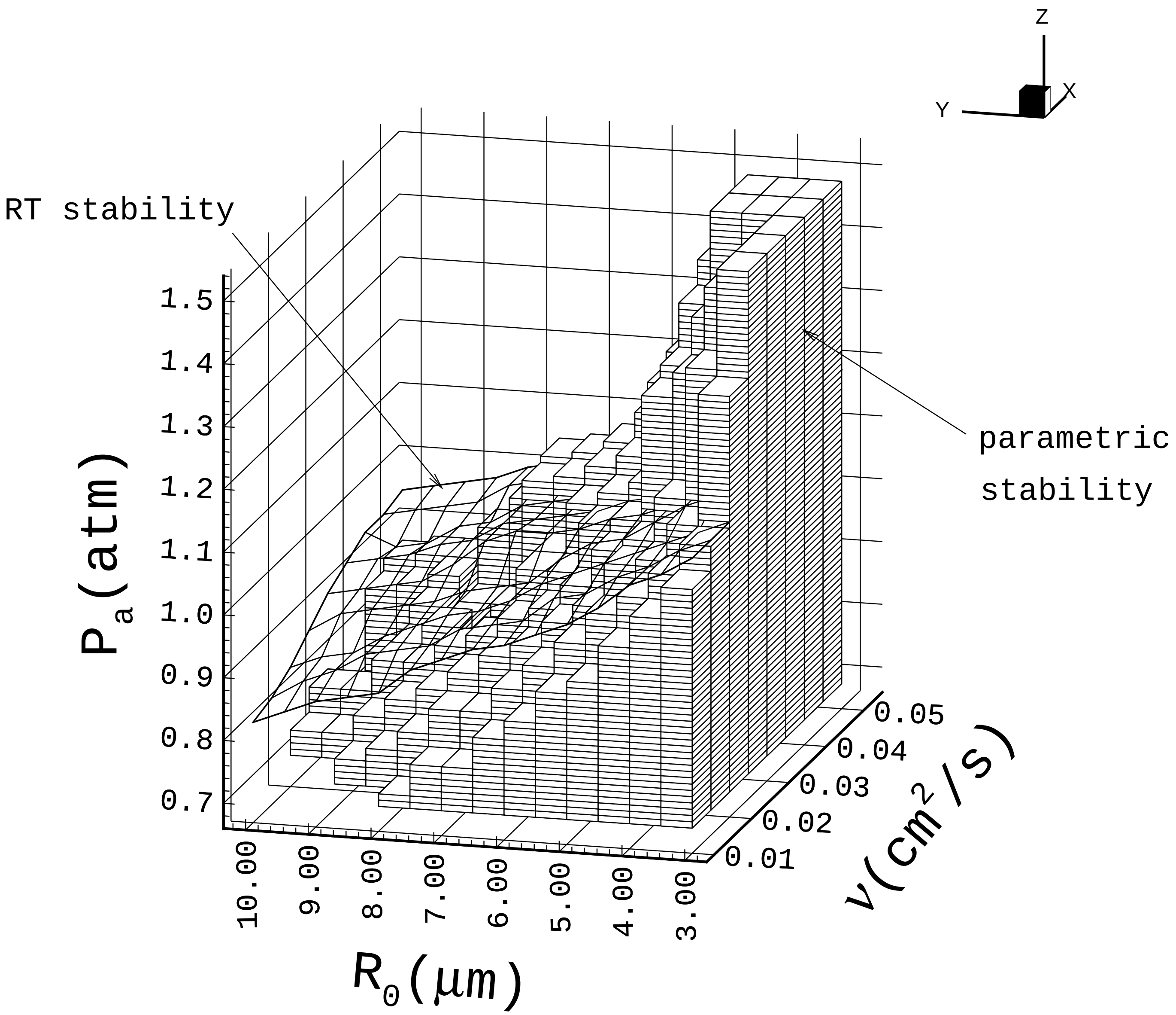
Z
Y
X
RT stability
parametric stability
1.5
1.4
1.3
1.2
1.1
1.0
0.9
0.8
0.7
P_a(atm)
10.00
9.00
8.00
7.00
6.00
5.00
4.00
3.00
$R_0(\mu m)$
0.05
0.04
0.03
0.02
0.01
$\nu(cm^2/s)$

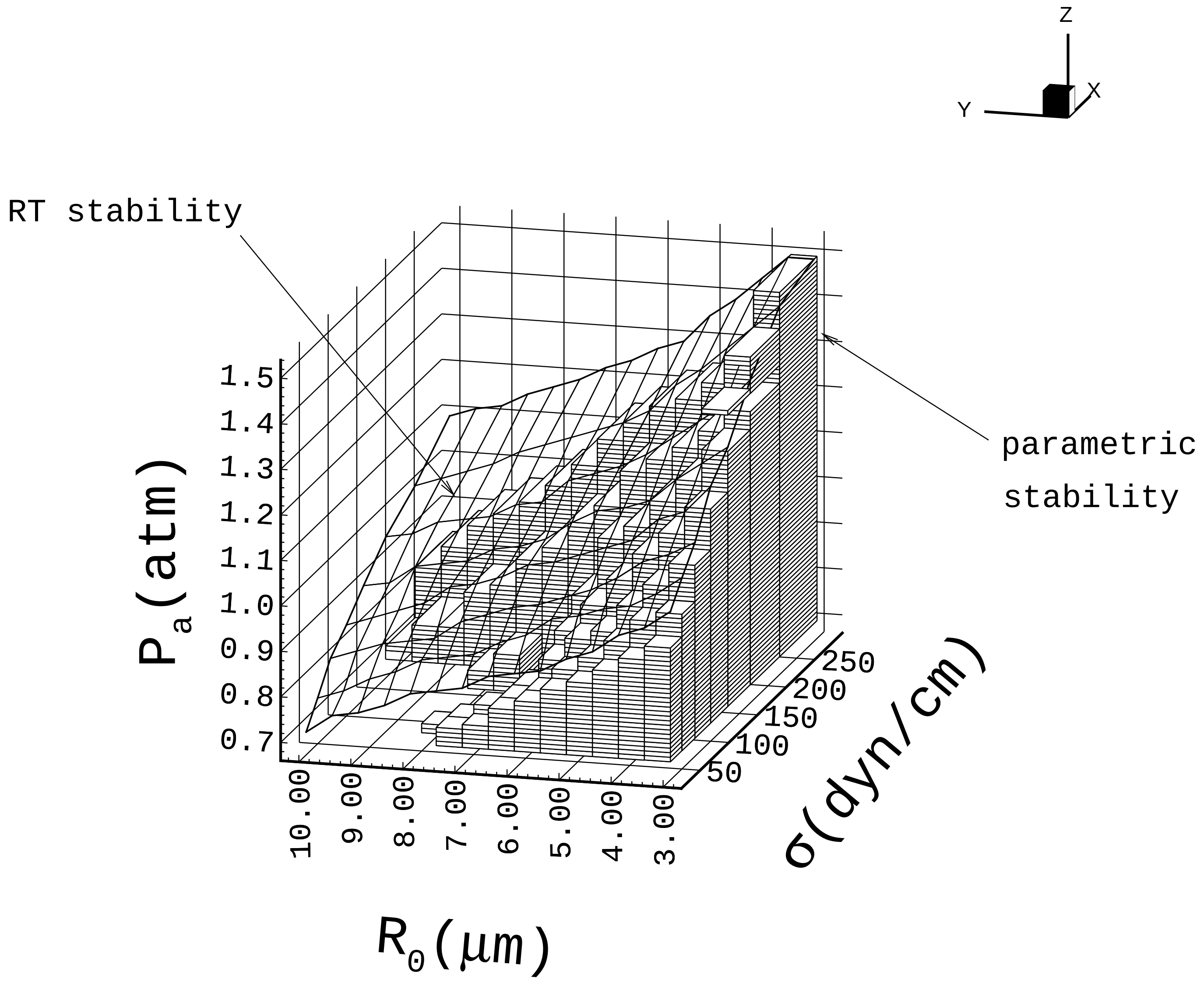
Z
Y
X
RT stability
parametric stability
1.5
1.4
1.3
1.2
1.1
1.0
0.9
0.8
0.7
Pa(atm)
10.00
9.00
8.00
7.00
6.00
5.00
4.00
3.00
R0(μm)
250
200
150
100
50
σ(dyn/cm)

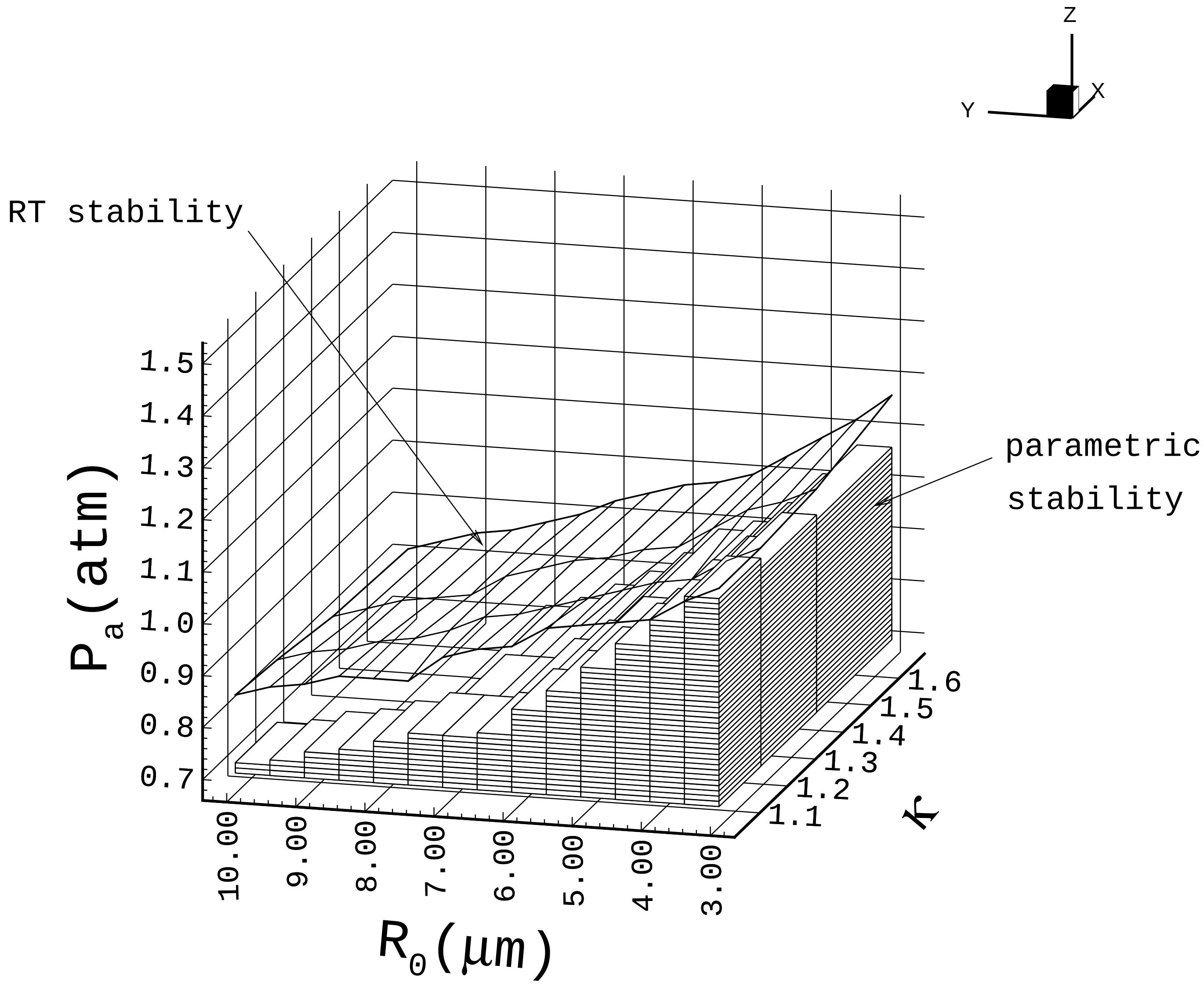

RT stability
parametric stability
Z
Y
X
1.5
1.4
1.3
1.2
1.1
1.0
0.9
0.8
0.7
P_a(atm)
10.00
9.00
8.00
7.00
6.00
5.00
4.00
3.00
$R_0(\mu m)$
1.1
1.2
1.3
1.4
1.5
1.6
κ